'$6Nb_2O_5.11WO_3$'

It was known that the powder X-ray diffractometer profile of '$6Nb_2O_5.11WO_3$' was very similar to that of $4Nb_2O_5.9WO_3$ (Roth & Waring, 1966), although a structure model has been proposed for this composition (Stephenson, 1968). Electron-microscopic observations (Iijima & Allpress, 1974; Obayashi & Anderson, 1976) could not provide any evidence of '$6Nb_2O_5.11WO_3$'. We have tried to solve the problem. Crystals with composition $6Nb_2O_5.11WO_3$ were prepared both at 1300 and 1250°C. They gave diffraction patterns and images very similar to those of $4Nb_2O_5.9WO_3$. Additional specimens with compositions $4Nb_2O_5.6WO_3$ and $5Nb_2O_5.5WO_3$ were prepared at 1300°C. It was expected from the phase diagram that the $9Nb_2O_5.8WO_3$ and $6Nb_2O_5.11WO_3$ phases coexist in both of them. The electron-microscopic observation revealed, however, the presence of $4Nb_2O_5.9WO_3$ together with $9Nb_2O_5.8WO_3$ (Roth & Wadsley, 1965). The same results were obtained from the specimens prepared at 1250°C with the same compositions, although $8Nb_2O_5.5WO_3$ and $6Nb_2O_5.11WO_3$ were expected from the phase diagram. It should be mentioned here that the reliability of the present temperature measurement is within 5°C. At any rate, it is important to note that there is no '$6Nb_2O_5.11WO_3$' phase. Fig. 8(*a*) shows a structure image of $9Nb_2O_5.8WO_3$ (tetragonal, $a = 26{\cdot}3$ and $c = 3{\cdot}81$ Å), prepared together with $4Nb_2O_5.9WO_3$ at 1250°C. It is clear on comparing with the structure model in Fig. 8(*b*) that the crystal is composed of 5×5 blocks. Each cation within the blocks is resolved as a dark spot. The cations in the octahedra sharing edges, as well as those in the sites of tetrahedral coordination, are shown in the image.

The authors wish to express their deep gratitude to Dr S. Yamaguchi, Dr Y. Bando and Mr Y. Sekikawa for their support of the present study.

References

ALLPRESS, J. G. (1972). *National Bureau of Standards Special Publication* 364, *Solid State Chemistry*, Proceedings of 5th Materials Research Symposium. Edited by R. S. ROTH & S. J. SCHNEIDER, pp. 87–111.

COWLEY, J. M. & MOODIE, A. F. (1957). *Acta Cryst.* **10**, 609–619.

CRAIG, D. C. & STEPHENSON, N. C. (1969). *Acta Cryst.* B**25**, 2071–2083.

CROMER, D. T. & WABER, J. T. (1965). *Acta Cryst.* **18**, 104–109.

FEJES, P. L. (1977). *Acta Cryst.* A**33**, 109–113.

HEIDENREICH, R. D. (1964). *Fundamentals of Transmission Electron Microscopy*, pp. 398. New York: Interscience.

HORIUCHI, S., KAWADA, I., NAKANO-ONODA, M., KATO, K., MATSUI, Y., NAGATA, F. & NAKAHIRA, M. (1976). *Acta Cryst.* A**32**, 558–565.

HORIUCHI, S., KIKUCHI, M. & GOTO, M. (1977). *Acta Cryst.* A**33**, 701–703.

HORIUCHI, S., MATSUI, Y. & BANDO, Y. (1976). *Jpn. J. Appl. Phys.* **15**, 2483–2484.

IIJIMA, S. & ALLPRESS, J. G. (1974). *Acta Cryst.* A**30**, 22–29.

OBAYASHI, H. & ANDERSON, J. S. (1976). *J. Solid State Chem.* **17**, 79–89.

SANGER, P. L. (1969). *Acta Cryst.* A**25**, 694–702.

SLEIGHT, A. W. (1966). *Acta Chem. Scand.* **20**, 1102–1112.

STEPHENSON, N. C. (1968). *Acta Cryst.* B**24**, 637–653.

ROTH, R. S. & WADSLEY, A. D. (1965). *Acta Cryst.* **19**, 38–41.

ROTH, R. S. & WARING, J. L. (1966). *J. Res. Natl Bur. Stand.* **70**A, 281–303.

Acta Cryst. (1978), A**34**, 946–949

A Simple Method for Obtaining Triclinic Cell Parameters from Weissenberg Photographs from One Crystal Setting

BY HANS HEBERT

Department of Medical Biophysics, Karolinska Institutet, S-104 01 Stockholm, Sweden

(*Received* 7 *April* 1978; *accepted* 24 *May* 1978)

A simple method is described for the interpretation of Weissenberg photographs and the determination of triclinic cell parameters from a single setting of the crystal. The theoretical approach is followed by an example illustrating the procedure. A comparison of these results with those derived from diffractometer measurements is made.

Introduction

Interpretation of Weissenberg photographs in the triclinic case is somewhat complicated by the lack of symmetry and the distorted pictures of the reciprocal lattice. When going to upper-level photographs the origins of the reciprocal-lattice levels are shifted from the rotation origin. The question is how these shifts show on Weissenberg films. If this transformation from reciprocal lattice to film is known, accurate measurements on the photographs can be used to determine the cell parameters. Buerger (1942) describes a method of angular lag, but his treatment suffers from two pronounced disadvantages. It requires two superposed Weissenberg exposures of the zero and first layers and, furthermore, the measurements are made on low-index reflexions which may be weak and unobservable. Another approach was made by Hulme (1966). His method involves measurements on general *hkl* reflexions. Two procedures for determining the cell parameters are described. One is geometrical which lowers the accuracy and the other is computational which requires computer facilities.

In the present method measurements are made on festoons representing either axes of the reciprocal lattice or lattice lines running parallel to these axes. The accuracy obtained for the angles finally derived is about $\pm 1°$. However, in the early stages of a structure determination one is often interested in a fast and easy method of obtaining preliminary unit-cell dimensions. The final parameters are then usually obtained from diffractometer measurements. The method is not applicable when split-film cassettes are employed, as is common for low-temperature work.

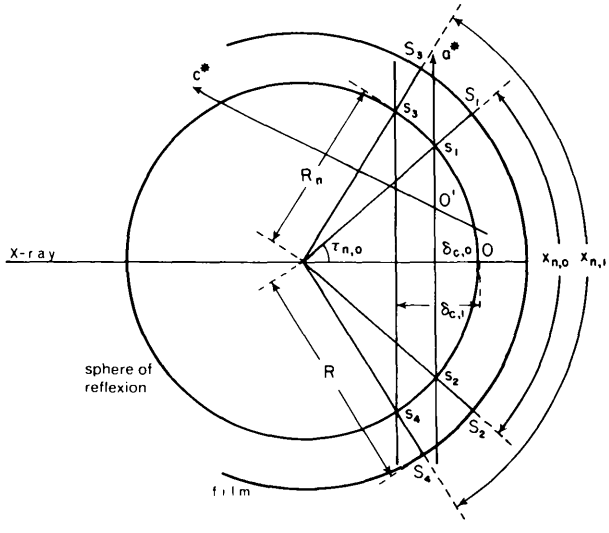

Fig. 1. A diagram of the nth layer for a crystal rotating about the b axis.

Outline of the procedure

Let a crystal rotate about an axis, say b, and study an upper level, say the *hnk* reflexions, by the equi-inclination Weissenberg technique. This situation is described in Fig. 1, where O is the true origin and rotation origin, while O' corresponds to the origin of the nth layer. When, for instance, the a^* axis of the reciprocal lattice is perpendicular to the entering X-ray beam, the points of intersection, s_1 and s_2, between the a^* axis and the sphere of reflexion will be symmetrically located with reference to the central X-ray line. On the film this will correspond to points S_1 and S_2 on the festoons representing the a^* axis. By measuring the distance between these points it is possible to determine the offset perpendicular to the a^* axis of the nth-layer origin from the true origin. With this distance and the layer-line separation, measured from an oscillation photograph, it is possible to calculate the angle α. Similarly, the angle γ may be obtained by measurements on the festoons corresponding to the c^* axis.

Theory

On the nth-layer Weissenberg film the distance between the symmetrically distributed points S_1 and S_2 is $x_{n,0}$. The geometry of Fig. 1 gives

$$\delta_{c,0} = R_n - R_n \cos \tau_{n,0} = R_n(1 - \cos \tau_{n,0}). \quad (1)$$

Now the angle $\tau_{n,0}$ (°) is given by

$$\tau_{n,0} = \frac{x_{n,0}}{2R} \times \frac{360}{2\pi}.$$

Furthermore, the radius R_n of the circle described by the intersection of the nth layer with the sphere of reflexion is $\cos \mu_n$ reciprocal-lattice units (r.l.u.), where μ_n is the equi-inclination angle of the nth layer. Thus (1) becomes (in r.l.u.)

$$\delta_{c,0} = \cos \mu_n \left[1 - \cos \left(\frac{x_{n,0}}{2R} \times \frac{360}{2\pi}\right)\right]. \quad (2)$$

However, by assuming the normal radius of the camera to be 28·65 mm the general expression above is simplified to

$$\delta_{c,0} = \cos \mu_n (1 - \cos x_{n,0}). \quad (3)$$

Now consider the reciprocal lattice in Fig. 2 where T is the projection of O' on to the a^*c^* plane. A line is drawn through this point perpendicular to the a^*b^* plane, thus corresponding to the direction of the c axis of the direct lattice. The angle between this line and TO', the direction of the b axis, will be α. By examining the triangle QTO' in Fig. 2 it is clear that the angle TQO' will be $180 - \alpha$. Thus

$$\tan (180 - \alpha) = -\tan \alpha = \frac{n\zeta_b}{\delta_{c,0}}, \quad (4)$$

where ζ_b is the layer-line separation. Similarly, γ is given by

$$\tan \gamma = -\frac{n\zeta_b}{\delta_{a,0}}, \qquad (5)$$

where $\delta_{a,0}$ is the offset of the nth-layer origin perpendicular to the c^* axis.

By applying the procedure to festoons corresponding to reciprocal-lattice lines parallel to the axes it is possible to obtain additional information and thereby increase the accuracy. For example, the measurement of $x_{n,1}$ in Fig. 1 will give (with $\delta_c = \delta_{c,0}$)

$$\delta_c = \delta_{c,1} - c^* \sin \beta^* = \cos \mu_n (1 - \cos x_{n,1}) - c^* \sin \beta^*,$$

where c^* and β^* are obtained from a zero-level photograph. Similarly, a general measurement $x_{n,i}$ corresponding to the intersection of the reciprocal-lattice line hni with the sphere of reflexion will give

$$\delta_c = \delta_{c,i} - ic^* \sin \beta^* \qquad (6)$$

and for δ_a

$$\delta_a = \delta_{a,i} - ia^* \sin \beta^*. \qquad (7)$$

However, the relations (6) and (7) may change owing to different choices of unit cells; this is illustrated in the example below. In general a Delaunay reduction (Delaunay, 1933; Patterson & Love, 1957; *International Tables for X-ray Crystallography*, 1952) may be applied to obtain the conventional triclinic cell.

Accuracy

Differentiation of expressions (3) and (4) gives

$$\mathrm{d}\delta_{c,0} = \cos \mu_n \sin x_{n,0}\, \mathrm{d}x_{n,0} \qquad (8)$$

$$\mathrm{d}\alpha = \frac{n\zeta_b}{\delta_{c,0}^2 + (n\zeta_b)^2}\, \mathrm{d}\delta_{c,0}. \qquad (9)$$

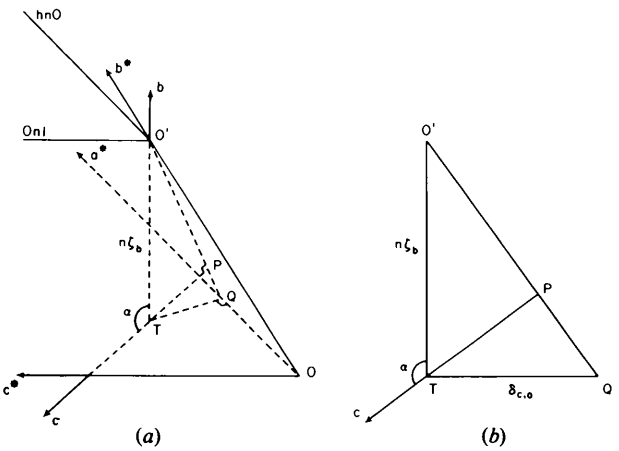

Fig. 2. (*a*) A general view of the reciprocal lattice. T is the projection of O' on to the a^*c^* plane. The line PT corresponds to the direction of the c axis. (*b*) The triangle QTO' on the plane of the paper.

The combination of these two equations gives an expression for the error in the final cell angle α

$$\mathrm{d}\alpha = \frac{n\zeta_b}{\delta_{c,0}^2 + (n\zeta_b)^2} \cos \mu_n \sin x_{n,0}\, \mathrm{d}x_{n,0}. \qquad (10)$$

An imagined structure with $b = 15$ Å and $\alpha = 100°$ will give (with $\lambda = 1{\cdot}5418$ Å and $n = 1$): $\zeta_b = 0{\cdot}1028$ r.l.u., $\mu_1 = 2{\cdot}95°$, $\delta_{c,0} = 0{\cdot}0181$ r.l.u. and $x_{1,0} = 10{\cdot}93$ mm. With these typical values (10) becomes

$$\mathrm{d}x_{1,0} = \frac{1}{1{\cdot}785}\, \mathrm{d}\alpha = 0{\cdot}56\, \mathrm{d}\alpha.$$

Thus to obtain a 1° accuracy in the final cell angle the distance $\mathrm{d}x_{1,0}$ must be accurate to about 0·5 mm. When it is possible to measure between reflexions situated directly above and below the axial intersection point this is a good estimate of the error. However, in the general case when festoon extrapolation has to be done, it can be difficult to keep errors within this limit especially if the reciprocal spacings are large.

An illustrative example

A recently studied compound, 2-methylamino-1-(spiro[cyclopentane-1,1′-inden]-3′-yl)ethanol hydrochloride, crystallizes in the triclinic space group $P\bar{1}$ (Hebert, 1978). To determine preliminary unit-cell dimensions the procedure described above was applied.

The results of these measurements for the second and third layers are in Table 1. The first layer was omitted because of too small deviations giving poor accuracy for the measurements. The rotation axis was denoted b and the length of this axis was 7·307 Å (determined from an oscillation photograph). The length of the a^* and c^* axes and the angle β^* were derived from measurements on a zero-layer Weissenberg photograph giving $a^* = 0{\cdot}0716$, $c^* = 0{\cdot}1368$ Å^{-1} and $\beta^* = 79{\cdot}17°$; Cu $K\alpha$ radiation ($\lambda = 1{\cdot}5418$ Å) was used. Fig. 3 is a schematic drawing of an upper-layer Weissenberg photograph indicating the measurements of $x_{n,i}$ and $y_{n,i}$. Note that the central line, easily obtained by letting the primary beam fall directly on the film, always bisects $x_{n,i}$ and $y_{n,i}$. These distances for the second and the third layers are in the second column of Table 1. Equation (3) with $\mu_2 = 12{\cdot}18°$ and $\mu_3 = 18{\cdot}45°$ gives $\delta_{c,i}$. The final δ_c values are then derived from $\delta_c = \delta_{c,i} - ic^* \sin \beta^*$ and equation (5) with $\zeta_b = 1/b = 0{\cdot}2110$ r.l.u. gives the angle α. The measurement of $y_{n,0}$ does not directly give the offset of the second and third-layer origins perpendicular to the c^* axis. This is because the intersection of this axis with the sphere of reflexion is not recorded on the photograph. This can be seen, for instance, from the fact that δ_a values decrease when derived from higher layers. However, reciprocal-lattice lines parallel to the c^* axis can be used as indicated in Fig. 4. Thus δ_a is given by $\delta_a = \delta_{a,i} - (i$

Table 1. *Angles α and γ derived from measurements on the second and third-layer equi-inclination Weissenberg photographs*

i	$x_{n,i}$	$\delta_{c,i}$	δ_c	α	$y_{n,i}$	$\delta_{a,i}$	δ_a	γ
2nd layer, $n = 2$, $\mu_2 = 12{\cdot}18°$								
0	10·2	0·0154	0·0154	92·09°	22·7	0·0757	0·0327	94·43°
1	39·3	0·2211	0·0139	91·89	35·1	0·1778	0·0390	95·28
2	55·8	0·4281	0·0137	91·86	45·3	0·2899	0·0353	94·78
3	69·5	0·6352	0·0135	91·83	53·5	0·3961	0·0375	95·08
3rd layer, $n = 3$, $\mu_3 = 18{\cdot}45°$								
0	11·8	0·0200	0·0200	91·81	20·5	0·0601	0·0483	94·36
1	40·3	0·2251	0·0179	91·62	34·2	0·1640	0·0528	94·77
2	57·0	0·4320	0·0176	91·59	44·0	0·2662	0·0590	95·32
3	71·0	0·6398	0·0181	91·64	52·5	0·3711	0·0625	95·64

+ 1)a^* sin β^*. Finally, equation (6) gives the angle γ. All the resulting cell parameters in both direct and reciprocal space are given in Table 2 together with the final parameters derived from diffractometer measurements. The latter were obtained by least-squares refinement of the setting angles of 25 accurately centred reflexions recorded on a Philips PW 1100 diffractometer.

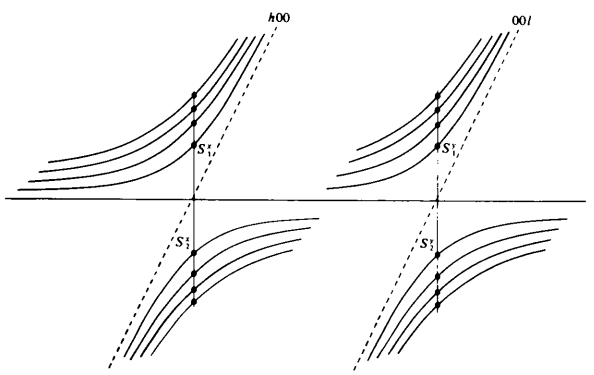

Fig. 3. Schematic drawing of an upper-layer equi-inclination Weissenberg photograph. $x_{n,0}$ and $y_{n,0}$ are the distances $S_1^x - S_2^x$ and $S_1^y - S_2^y$ respectively. Similarly, $x_{n,1}$ and $y_{n,1}$ are the distances between the ith-order festoons.

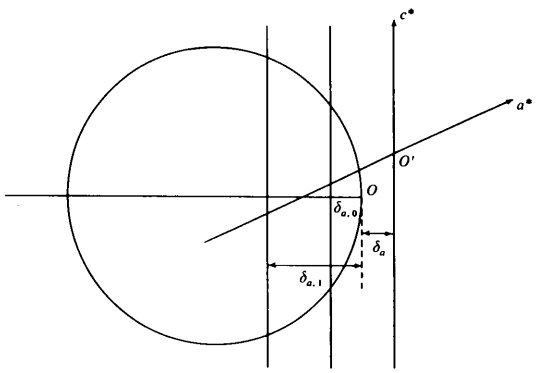

Fig. 4. An illustration of the relations between various shifts.

Table 2. *Direct and reciprocal unit-cell parameters for 2-methylamino-1-(spiro[cyclopentane-1,1′-inden]-3′-yl)ethanol hydrochloride obtained from Weissenberg photographs and diffractometer measurements*

Weissenberg				Diffractometer			
a =	14·27 Å	a^* =	0·0716 Å^{-1}	a =	14·137 Å	a^* =	0·0722 Å^{-1}
b =	7·31	b^* =	0·1375	b =	7·324	b^* =	0·1370
c =	7·44	c^* =	0·1368	c =	7·430	c^* =	0·1371
α =	91·8°	α^* =	87·25°	α =	92·06°	α^* =	87·13°
β =	100·5	β^* =	79·17	β =	100·63	β^* =	79·19
γ =	95·0	γ^* =	84·62	γ =	94·10	γ^* =	85·44

With the cell parameters derived in this manner a right-handed coordinate system cannot be found together with the condition that all the angles of the direct cell have to be greater than 90°. However, if an alternative b^* axis is chosen along a diagonal in the a^*b^* plane the above requirements are fulfilled. The cell parameters found with this choice of b^* axis can also be derived directly by calculating δ_a values from $\delta_a = \delta_{a,i} - (i - 1)a^*$ sin β^*.

References

BUERGER, M. J. (1942). *X-ray Crystallography*, p. 377 ff. New York: John Wiley.

DELAUNAY, B. (1933). *Z. Kristallogr.* **84**, 132.

HEBERT, H. (1978). *Acta Cryst.* B**34**, 3128–3131.

HULME, R. (1966). *Acta Cryst.* **21**, 898–900.

International Tables for X-ray Crystallography (1952). Vol. I, p. 530. Birmingham: Kynoch Press.

PATTERSON, A. L. & LOVE, W. E. (1957). *Acta Cryst.* **10**, 11.